Taylor & Francis
Taylor & Francis Group

International Journal of Control

ISSN: (Print) (Online) Journal homepage: https://www.tandfonline.com/loi/tcon20

Adaptive backstepping-based sampled-data tracking control with prescribed performance for switched nonlinear systems

Si-Min Liu, Shan-Liang Zhu & Yu-Qun Han

INTERNATIONAL JOURNAL OF CONTROL
https://doi.org/10.1080/00207179.2023.2241921

Adaptive backstepping-based sampled-data tracking control with prescribed performance for switched nonlinear systems

Si-Min Liu [a], Shan-Liang Zhu [a,b] and Yu-Qun Han [a,b]

[a]School of Mathematics and Physics, Qingdao University of Science and Technology, Qingdao, People's Republic of People's Republic of China; [b]The Research Institute for Mathematics and Interdisciplinary Sciences, Qingdao University of Science and Technology, Qingdao, People's Republic of China

ABSTRACT
In this paper, the problem of sampled-data adaptive tracking control for a class of switched nonlinear systems with prescribed performance is considered. In order to guarantee the system is stable and achieves the prescribed performance in sampled-data control, a coordinate transformation satisfying the prescribed performance is introduced. In addition, the neural networks (NNs) used to approximate the unknown nonlinear functions and the backstepping technique are applied to design the sampled-data controller and the adaptive laws. An upper bound on the sampling period is obtained to maintain the stability of the systems. It is confirmed that the designed sampled-data scheme ensures that all signals of the closed-loop system are semi-globally uniformly ultimately bounded (SGUUB) and the tracking error is limited to the prescribed performance function. The effectiveness of the designed control scheme is demonstrated by two simulation examples.

ARTICLE HISTORY
Received 28 October 2022
Accepted 24 July 2023

KEYWORDS
Sampled-data control; prescribed performance; switched nonlinear systems; adaptive control; neural networks

1. Introduction

Many industrial systems can be described as switched systems, such as electrical systems (Wu et al., 2018), flight control systems (Jin et al., 2014), and mechanical engineering systems (Ma et al., 2020). So far, many interesting results based on adaptive control have been explored for different types of switched systems, such as switched nonlinear systems (Zhang & Wei, 2021), stochastic switched systems (Niu et al., 2018), switched large-scale systems (Ma & Ma, 2020), and switched multi-agent systems (Li & Zhao, 2021). Since the stability of the switched nonlinear systems is affected by the combination of the switching signals and the stability of subsystems, common Lyapunov functions (CLFs) (Liu et al., 2022; Zeng et al., 2021), multiple Lyapunov functions (MLFs) (Chen et al., 2021; Niu, Liu, et al., 2020), and average dwell time (ADT) (Cui et al., 2022; Liu et al., 2021) are often applied to study switched nonlinear systems. Among them, the CLFs-based method can ensure the switched nonlinear system remains stable under any switching signal. Therefore, many adaptive control strategies have been proposed (Lai et al., 2018; Niu, Wang, et al., 2020). However, if there are unknown complex nonlinear structures in switched nonlinear systems, adaptive control faces the dilemma of method failure and performance degradation. To address this problem, many approximation methods, such as fuzzy logic systems (FLSs) and neural networks (NNs), have been extensively applied to solve the control problem of nonlinear systems, which can greatly remove the limitations of the backstepping technique. As a result, combining approximation-based method with the adaptive backstepping control technique, many control strategies have been reported for switched nonlinear systems. For example, Zeng et al. (2021) proposed an adaptive neural tracking control approach for uncertain switched nonlinear systems with state quantisation. Liu et al. (2022) solved the problem of full-state constraints with the help of FLSs. Meng et al. (2020) proposed an adaptive fault-tolerant control scheme via FLSs and backstepping methods. However, most of these control strategies for switched nonlinear systems have focused on continuous-time control, which cannot be directly applied to practical computer control systems.

Sampled-data control has increasingly been studied because of its more intelligent and higher flexibility, which has been widely applied in active suspension systems (Li, Xie, et al., 2021) and electric power market (Zhang & Xiao, 2020). The key idea of sampled-data control is to sample the information of the continuous control systems periodically or randomly. And then, the control input is obtained at the sampling moment. In other words, the control input is a right continuous segmentation function with time intervals of twice sampling moments. Therefore, the sampled-data control only requires information at the moment of sampling time and does not require real-time feedback, reducing the information transmission burden. In recent years, researches on the problems of sampled-data control have become increasingly diverse (Guan et al., 2022; Sheng et al., 2022; Su et al., 2018). Many interesting results have been obtained for the problem of sampled-data control. For example, Sheng et al. (2022) proposed a novel Lyapunov functional method to guarantee the stability of linear sampled-data systems in the case of aperiodic sampling. Moreover, for the sampled-data control of nonlinear systems, the continuous-time plant model plus controller discretisation (CTD) method has been

CONTACT Yu-Qun Han yuqunhan@163.com School of Mathematics and Physics, Qingdao University of Science and Technology, Qingdao 266061, People's Republic of China

one of the popular methods. As it can be derived from the strategies and ideas of designing continuous-time controllers and is simple to comprehend, many results have been emerged. For examples, Li & Yu (2022) developed a sampled-data control strategy for non-strict feedback large-scale interconnected systems with completely unknown nonlinear functions and states. Li, Ahn, et al. (2021) investigated the stabilisation problem of switched nonlinear systems with sampled-data control. Although there have been many remarkable results for the study of sampled-data control, few results involved prescribed performance control.

In fact, it's not enough to only considering the stability of the system in the practical. Given the prescribed performance control, especially its ability in transient and steady of the system, it shows widespread attention in the control problem (Li et al., 2018; Li et al., 2017; Li & Tong, 2015; Sui et al., 2015; Tang & Zhao, 2017; Wang, Zou, et al., 2018; Zhu & Han, 2022). Among them, Wang, Zou, et al. (2018) studied the prescribed performance control problem for nonlinear systems. Zhu & Han (2022) proposed an adaptive prescribed performance control method for large-scale nonlinear systems with asymmetric input saturation. Li et al. (2018) proposed a control scheme for nonlinear systems with sampled-data control and prescribed performance control. Furthermore, Ming et al. (2017) applied prescribed performance control to air-breathing supersonic missiles and proposed a fault-tolerant control scheme based on sliding mode control. Huang et al. (2015) developed the prescribed performance control to the vehicle suspension system to balance the suspension's smoothness and the vehicle's safety. Although there have been quite many achievements of prescribed performance control, to the best of the authors' knowledge, the few efforts have been devoted to the adaptive sampled-data tracking control for switched nonlinear systems under prescribed performance.

Inspired by the research mentioned above, this paper studies the problem of sample-data control for a class of switched nonlinear systems with prescribed performance. The radial basis function neural networks (RBFNNs) are used to approximate the unknown nonlinear functions. Then, an adaptive sampled-data tracking control scheme is proposed based on backstepping technique. The proposed approach can ensure the closed-loop system semi-globally uniformly ultimately bounded (SGUUB) and the tracking error achieves the prescribed performance requirements. In contrast to the existing research results, the main contributions of this paper are summarised as follows:

(1) It is the first time to consider sampled-data tracking control with prescribed performance for a class of switched nonlinear systems. A novel adaptive sampled-data control scheme is proposed with the information sampled periodically, which can greatly reduce the computational load and the burden of transmission information.
(2) Compared with the available results (Li et al., 2017; Tang & Zhao, 2017; Wang, Zou, et al., 2018), which merely focus on the application of prescribed performance control in continuous-time control processes, our study will design a discrete controller in the switched nonlinear system based on sampling information. The structure of the designed controller is more simplicity and more reliable. Meanwhile, it also guarantees that all signals are SGUUB and the tracking error is always limited to the range of performance function.
(3) In contrast to the sampled-data control-based prescribed performance control method proposed in (Li et al., 2018), which mainly focues on nonlinear systems. In this paper, the sampled-data control with prescribed performance is extended the tracking problem of switched nonlinear systems.

2. Problem formulation and preliminaries

2.1 System and control objective

In this paper, the following switched nonlinear systems containing multiple subsystems are considered

$$\begin{cases} \dot{x}_i = x_{i+1} + f_{i,\sigma(t)}(\bar{x}_i) \\ \;\; i = 1, 2, \ldots, n-1 \\ \dot{x}_n = u + f_{n,\sigma(t)}(x) \\ \;\; y = x_1 \end{cases} \tag{1}$$

where $x_1, \cdots, x_n$ denote the system states, $\bar{x}_i = [x_1, \cdots, x_i]^{\mathrm{T}} \in R^i$ for $i = 1, \cdots, n$. $\sigma(t) : [0, \infty) \to \mathbb{N} = \{1, 2, \cdots, N\}$ denotes the switching signal with N being the N - th subsystems. $f_{i,l}(\cdot), l \in \mathbb{N}$ denotes an unknown continuous nonlinear function with $f_{i,l}(0) = 0$. T denotes the sampling period, then $t_k = kT$ and t_{k+1} are discrete sampling moments. $u \in R$ denotes the sampled-data controller, where $u(t) = u(t_k), \forall t \in [t_k, t_{k+1})$, $k = 0, 1, 2, \cdots$. $y \in R$ denotes the system output. In this paper, the system state does not jump at the switching instant.

To better understand the objectives of this paper, the following definition of SGUUB needs to be introduced.

Definition 2.1 (Li, Ahn, et al., 2019): Consider the nonlinear system described by $\dot{x} = f(x), x, f(x) \in R^n$. If for any compact subset $\Lambda \in R^n$ and state $x(t_0) = x_0 \in \Lambda$, there exist $\varepsilon > 0$ and $\delta(\varepsilon, x_0)$, which satisfy $||x(t)|| \leq \varepsilon, \forall t > t_0 + \delta$. Then the solution of the system is SGUUB.

Consider the switched nonlinear systems (1), the objective of this study is to design an adaptive sampled-data control strategy that can achieve the following goals:

(i) All signals of system (1) are SGUUB under any switching signal.
(ii) The output signal y can effectively track the reference signal y_d. Meanwhile, the tracking error is limited to the given prescribed performance range.

The following assumptions and lemmas are needed for the convenience of control strategy design.

Assumption 2.1: All states of the switched nonlinear system (1) are measured only at the sampling moment, which can be used to design the adaptive sampled scheme.

Remark 2.1: It is important to note that the system (1) can be regarded as an abstract expression of the system model of many practical systems, such as the single-link robotic manipulator (Lian & Li, 2020), the mass-spring damper (MSD) (Wang & Long, 2022; Zhai et al., 2018), the continuous stirred tank reactor (CSTR) (Liu et al., 2022), etc. Thus, the research of system (1) has very important practical meaning and applicable value.

Remark 2.2: In the practical control process, it is more flexible to use digital controllers. However, digital controllers can't obtain the real-time state of the continuous system, instead relying on the sampling time to acquire the instantaneous state of the system. Therefore, Assumption 2.1 is widely used in sampled-data control.

In the tracking control process, the reference signal y_d needs to be considered.

Assumption 2.2: The reference signal y_d is a continuous function and differentiable of order n.

Lemma 2.1 (Li, Guo, et al., 2019): *Consider a real region $G := [a,b] \subset R$, there exist real continuous functions $v(t)$, $w(t)$ and $\tau(t) \geq 0$ defined in the region G. The following inequality holds for $\forall t \in G$*

$$v(t) \leq w(t) + \int_a^t w(s)\tau(s)e^{\int_s^t \tau(r)dr} ds$$

if $v(t)$ satisfies the following inequality

$$v(t) \leq w(t) + \int_a^t \tau(s)v(s)ds$$

2.2 Prescribed performance function

The idea of prescribed performance control is introduced to achieve the objective (ii), which can limit the tracking error within a specific range. Firstly, a time-variable gain function $\iota(t)$ is introduced to describe the control input

$$u(t) = \iota(\phi(t), m(t), ||y(t) - y_d(t)||)(y(t) - y_d(t))$$

where $\phi(t)$ is the boundary function, $m(t)$ is the scaling function with $m(t) = \frac{1}{\rho(t)}$ and $||y(t) - y_d(t)||$ is the Euclidian norm of the tracking error.

Secondly, introduce a new function as follows

$$D(t) = \rho(t) - ||y(t) - y_d(t)||$$

where $D(t)$ denotes the vertical distance between $\rho(t)$ and $||y(t) - y_d(t)||$. Therefore, the time-varying gain $\iota(t)$ is given as

$$\iota(t) = \frac{m(t)}{D(t)} = \frac{m(t)}{\rho(t) - ||y(t) - y_d(t)||} \tag{2}$$

Then, the prescribed performance function $\phi(t)$ is designed as

$$\phi(t) = (\phi_0 - \phi_\infty)e^{-\lambda t} + \phi_\infty$$

where ϕ_0 is the initial value of $\phi(t)$. ϕ_∞ is the limit of the performance function at the steady state with $\phi_\infty = \lim_{t\to\infty} \phi(t)$. λ is the rate of convergence of the exponential function. ϕ_0, ϕ_∞, λ are pre-designed positive constants. The prescribed performance is satisfied when the tracking error reaches the control target $-\phi(t) < y(t) - y_d(t) < \phi(t)$.

Finally, according to Wang, Zou, et al., 2018; Zhu & Han (2022), the following coordinate transformation is designed to accomplish the performance goal

$$\xi(t) = \frac{(y(t) - y_d(t))^2}{\phi^2(t) - (y(t) - y_d(t))^2} \tag{3}$$

Meanwhile, according to (3), we can also obtain

$$\dot{\xi}(t) = 2\varsigma\left(\dot{y} - \dot{y}_d - y\frac{\dot{\phi}}{\phi}\right) \tag{4}$$

where $\varsigma = \frac{(y(t)-y_d(t))\phi^2}{(\phi^2-(y(t)-y_d(t))^2)^2}$.

Remark 2.3: According to the equation (2), it is obvious that if the tracking error converges to $\phi(t)$, the time-varying gain $\iota(t)$ will increase. Therefore, the prescribed performance control can guarantee a prescribed transient behaviour.

2.3 RBFNN

In this paper, RBFNNs are used to deal with the unknown smooth nonlinear functions.

Lemma 2.2 (Sanner & Slotine, 1992): *Considering an unknown smooth nonlinear function $f(X): R^n \to R$ defined on a closed interval $\Omega_X \subset R^n$, for $\forall\delta^* > 0$, there exists a RBFNN such that*

$$f(X) = W^{*\mathrm{T}}H(X) + \delta(X)$$

where $X \in \Omega_X \subset R^n$ denotes the input vector with n being input dimension, $W^* = [W_1, W_2, \cdots, W_m]^{\mathrm{T}} \in R^m$ denotes the ideal weight vector, m denotes the number of nodes in the hidden layer of the neural network, $H(X) = [h_1(X), h_2(X), \cdots, h_m(X)]^{\mathrm{T}}$ denotes the Gaussian basis function, and $\delta(X)$ denotes the approximation error and satisfies $|\delta(X)| < \delta^*$.

Remark 2.4: It is theoretically possible to approximate the nonlinear function with arbitrary accuracy with a sufficient number of hidden nodes and sufficient learning. Therefore, RBFNNs are suitable for solving the control problems in nonlinear systems with complex nonlinearity (Wang, Chen, et al., 2018; Zhang et al., 2021). Since RBFNN has the advantages of self-study ability and fast calculation, the RBFNN-based control algorithm demonstrates excellent control performance with a simple structure.

3. Main results

Before controller design, the following coordinate transformation is introduced:

$$\begin{cases} z_1 = x_1 - y_d \\ z_i = x_i - \alpha_{i-1}, i = 2, \cdots, n \end{cases} \tag{5}$$

where α_{i-1} denotes the virtual control signal, which will be designed later.

3.1 Sampled-data controller design

If $\forall t \in [t_k, t_{k+1})$, the $l-th$ subsystem is activated and $\sigma(t_k) = l, l \in \mathbb{N}$.

Step 1: The following Lyapunov function is considered

$$V_1 = \frac{1}{4}\xi^2 + \sum_{j=1}^{N} \frac{\tilde{\theta}_{1,j}^{\mathrm{T}}\tilde{\theta}_{1,j}}{2}$$

where $\tilde{\theta}_{1,j} = \theta_{1,j} - \hat{\theta}_{1,j}$ is the parameter estimation error of RBFNN, $\theta_{1,j}$ and $\hat{\theta}_{1,j}$ are the weight vector and its estimation.

By taking the derivative of V_1, we have

$$\dot{V}_1 = \xi\left(\varsigma z_2 + \varsigma\alpha_1 + \varsigma f_{1,l} - \varsigma\dot{y}_d - \varsigma x_1\frac{\dot{\phi}}{\phi}\right) - \sum_{j=1}^{N}\tilde{\theta}_{1,j}^{\mathrm{T}}\dot{\hat{\theta}}_{1,j}$$

$$= \xi(\varsigma z_2 + \varsigma\alpha_1 + F_{1,l}) - \sum_{j=1}^{N}\tilde{\theta}_{1,j}^{\mathrm{T}}\dot{\hat{\theta}}_{1,j} \tag{6}$$

where $F_{1,l} = \varsigma f_{1,l} - \varsigma\dot{y}_d - \varsigma x_1\frac{\dot{\phi}}{\phi}$.

Obviously, $F_{1,l}$ is an unknown nonlinear function, which cannot be directly used for controller design. Therefore, according to Lemma 2.2, $F_{1,l}$ can be approximated by a RBFNN with the following form

$$F_{1,l}(S_1) = \theta_{1,l}^{\mathrm{T}}P_1(S_1) + \delta_{1,l}(S_1) \quad l \in \mathbb{N} \tag{7}$$

where $S_1 = [x_1]^{\mathrm{T}}$, $\theta_{1,l}$ is the ideal weight vector and $\delta_{1,l}$ is the approximation error satisfying $|\delta_{1,l}(S_1)| \le \delta_{1,l}^*$ with $\delta_{1,l}^*$ being a positive constant.

Substituting (7) into (6), we have

$$\dot{V}_1 \le \xi\varsigma z_2 + \xi\varsigma\alpha_1 + \xi\theta_{1,l}^{rmT}P_1(S_1) + \xi\delta_{1,l} - \sum_{j=1}^{N}\tilde{\theta}_{1,j}^{\mathrm{T}}\dot{\hat{\theta}}_{1,j} \tag{8}$$

According to (8), the virtual control signal α_1 and adaptive control law $\dot{\hat{\theta}}_{1,l}(t)$ are constructed as follows

$$\alpha_1 = -\frac{1}{\varsigma}\left(\mu_1\xi + \sum_{j=1}^{N}\hat{\theta}_{1,j}^{\mathrm{T}}P_1(S_1)\right) \tag{9}$$

$$\dot{\hat{\theta}}_{1,l}(t) = \omega_{l,\sigma(t)}(\xi(t_k)P_1(S_1(t_k)) - \sigma_{1,l}\hat{\theta}_{1,l}(t)) \tag{10}$$

where μ_1 and $\sigma_{1,l}$ are positive design parameters, and $\omega_{l,j} = \begin{cases} 0, l \ne j \\ 1, l = j \end{cases}$.

Furthermore, it follows from (8) and (10) that

$$\sum_{j=1}^{N}\tilde{\theta}_{1,j}^{\mathrm{T}}\dot{\hat{\theta}}_{1,j} \le \tilde{\theta}_{1,l}^{\mathrm{T}}\xi(t_k)P_1(S_1(t_k)) - \sigma_{1,l}\tilde{\theta}_{1,l}^{\mathrm{T}}\theta_{1,l}(t)$$
$$+ \sum_{j=1}^{N}\sigma_{1,j}\tilde{\theta}_{1,j}^{\mathrm{T}}\tilde{\theta}_{1,j}(t) - \sum_{j=1,j\ne l}^{N}\sigma_{1,j}\tilde{\theta}_{1,j}^{\mathrm{T}}\tilde{\theta}_{1,j}(t) \tag{11}$$

Then, substituting (9), (10), and (11) into (8), yields

$$\dot{V}_1 \le -\mu_1\xi^2 + \xi\varsigma z_2 + 2\sqrt{V_1(t)}\sum_{j=1,j\ne l}^{N}(|\theta_{1,j}| + |\tilde{\theta}_{1,j}|)$$
$$+ 2\sqrt{V_1(t)}\delta_{1,l}^* + \sqrt{2}\sqrt{V_1(t)}|\xi - \xi(t_k)|$$
$$+ 4\sqrt{2}\sqrt{V_1(t)}\sqrt{V_1(t_k)} + \sqrt{2}\sqrt{V_1(t)}\sigma_{1,l}|\theta_{1,l}|$$
$$- \sum_{j=1}^{N}\sigma_{1,j}\tilde{\theta}_{1,j}^{\mathrm{T}}\tilde{\theta}_{1,j} + \sqrt{2}\sqrt{V_1(t)}\sum_{j=1,j\ne l}^{N}\sigma_{1,j}|\tilde{\theta}_{1,j}|$$
$$\le -\mu_1\xi^2 + \xi\varsigma z_2 - \sum_{j=1}^{N}\sigma_{1,j}\tilde{\theta}_{1,j}^{\mathrm{T}}\tilde{\theta}_{1,j} + \sqrt{2}\sqrt{V_1(t)}|\xi - \xi(t_k)|$$
$$+ 4\sqrt{2}\sqrt{V_1(t)}\sqrt{V_1(t_k)} + \zeta_{1,l}\sqrt{V_1(t)} \tag{12}$$

where

$$\zeta_{1,l} = \sqrt{2}\left(\sqrt{2}\sum_{j=1,j\ne l}^{N}(|\theta_{1,j}| + |\tilde{\theta}_{1,j}|) + \sigma_{1,l}|\theta_{1,l}| + \sum_{j=1,j\ne l}^{N}\sigma_{1,j}|\tilde{\theta}_{1,j}| + \sqrt{2}\delta_{1,l}^*\right).$$

Step 2: Similar to the Step 1, considering the following Lyapunov function

$$V_2 = V_1 + \frac{1}{2}z_2^2 + \sum_{j=1}^{N}\frac{\tilde{\theta}_{2,j}^{\mathrm{T}}\tilde{\theta}_{2,j}}{2}$$

where $\tilde{\theta}_{2,j} = \theta_{2,j} - \hat{\theta}_{2,j}$ is the parameter estimation error of RBFNN, $\theta_{2,j}$ and $\hat{\theta}_{2,j}$are the weight vector and its estimation.

By taking the derivative of V_2, we have

$$\dot{V}_2 = \dot{V}_1 + z_2z_3 + z_2\alpha_2 + z_2f_{2,l} - z_2\dot{\alpha}_1 - \sum_{j=1}^{N}\tilde{\theta}_{2,j}^{\mathrm{T}}\dot{\hat{\theta}}_{2,j}$$

$$= \dot{V}_1 + \frac{1}{2}z_3^2 + z_2\alpha_2 + z_2F_{2,l} - \xi\varsigma z_2 - \sum_{j=1}^{N}\tilde{\theta}_{2,j}^{\mathrm{T}}\dot{\hat{\theta}}_{2,j} \tag{13}$$

where $F_{2,l} = \xi\varsigma + \frac{1}{2}z_2 + f_{2,l} - \dot{\alpha}_1$.

Obviously, $F_{2,l}$ is an unknown nonlinear function, which cannot be directly used for controller design. Therefore, according to Lemma 2.2, $F_{2,l}$ can be approximated by a RBFNN with the following form

$$F_{2,l}(S_2) = \theta_{2,l}^{\mathrm{T}}P_2(S_2) + \delta_{2,l}(S_2) \quad l \in \mathbb{N} \tag{14}$$

where $S_2 = [x_1, x_2, \hat{\theta}_{1,1}, \cdots, \hat{\theta}_{1,N}]^{\mathrm{T}}$, $\theta_{2,l}$ is the ideal weight vector and $\delta_{2,l}$ is the approximation error satisfying $|\delta_{2,l}(S_2)| \le \delta_{2,l}^*$ with $\delta_{2,l}^*$ being a positive constant.

Substituting (14) into (13), we have

$$\dot{V}_2 \le \dot{V}_1 + \frac{1}{2}z_3^2 + z_2\alpha_2 + z_2\theta_{2,l}^{\mathrm{T}}P_2(S_2)$$

$$+ z_2\delta_{2,l} - \xi\varsigma z_2 - \sum_{j=1}^{N}\tilde{\theta}_{2,j}^{\mathrm{T}}\dot{\hat{\theta}}_{2,j} \tag{15}$$

According to (15), the virtual control signal α_2 and adaptive control law $\dot{\hat{\theta}}_{2,l}(t)$ are constructed as follows

$$\alpha_2 = -\mu_2 z_2 - \sum_{j=1}^{N}\hat{\theta}_{2,j}^{\mathrm{T}} P_2(S_2) \tag{16}$$

$$\dot{\hat{\theta}}_{2,l}(t) = \omega_{l,\sigma(t)}(z_2(t_k)P_2(S_2(t_k)) - \sigma_{2,l}\hat{\theta}_{2,l}(t)) \tag{17}$$

where μ_2 and $\sigma_{2,l}$ are design positive parameters.

Furthermore, it follows from (15) and (17) that

$$\sum_{j=1}^{N}\tilde{\theta}_{2,j}^{\mathrm{T}}\dot{\hat{\theta}}_{2,j} \le \tilde{\theta}_{2,l}^{\mathrm{T}} z_2(t_k)P_2(S_2(t_k)) - \sigma_{2,l}\tilde{\theta}_{2,l}^{\mathrm{T}}\theta_{2,l}(t) + \sum_{j=1}^{N}\sigma_{2,j}\tilde{\theta}_{2,j}^{\mathrm{T}}\tilde{\theta}_{2,j}(t) - \sum_{j=1,j\neq l}^{N}\sigma_{2,j}\tilde{\theta}_{2,j}^{\mathrm{T}}\tilde{\theta}_{2,j}(t) \tag{18}$$

Then, substituting (16), (17), and (18) into (15), yields

$$\begin{aligned}
\dot{V}_2 \le{}& \dot{V}_1 - \mu_2 z_2^2 + \frac{1}{2}z_3^2 + \sqrt{2}\sqrt{V_2(t)}\sum_{j=1,j\neq l}^{N}(|\theta_{2,j}| + |\tilde{\theta}_{2,j}|) \\
&+ \sqrt{2}\sqrt{V_2(t)}\delta_{2,l}^{*} + \sqrt{2}\sqrt{V_2(t)}|z_2 - z_2(t_k)| \\
&+ 4\sqrt{V_2(t)}\sqrt{V_2(t_k)} + \sqrt{2}\sqrt{V_2(t)}\sigma_{2,l}|\theta_{2,l}| \\
&- \sum_{j=1}^{N}\sigma_{2,j}\tilde{\theta}_{2,j}^{\mathrm{T}}\tilde{\theta}_{2,j} + \sqrt{2}\sqrt{V_2(t)}\sum_{j=1,j\neq l}^{N}\sigma_{2,j}|\tilde{\theta}_{1,j}| \\
\le{}& -\mu_1\xi^2 - \mu_2 z_2^2 + \frac{1}{2}z_3^2 - \sum_{i=1}^{2}\sum_{j=1}^{N}\sigma_{i,j}\tilde{\theta}_{i,j}^{\mathrm{T}}\tilde{\theta}_{i,j} \\
&+ \sqrt{2}\sqrt{V_2(t)}|\xi - \xi(t_k)| + \sqrt{2}\sqrt{V_2(t)}|z_2 - z_2(t_k)| \\
&+ \left(4\sqrt{2} + 4\right)\sqrt{V_2(t)}\sqrt{V_2(t_k)} + \zeta_{2,l}\sqrt{V_2(t)}
\end{aligned} \tag{19}$$

with $\zeta_{2,l} = \sqrt{2}\left(\sum_{j=1,j\neq l}^{N}(|\theta_{2,j}| + |\tilde{\theta}_{2,j}|) + \sigma_{2,l}|\theta_{2,l}| + \sum_{j=1,j\neq l}^{N}\sigma_{2,j}|\tilde{\theta}_{2,j}| + \delta_{2,l}^{*}\right) + \zeta_{1,l}$.

Step $\rho(3 \le \rho \le n-1)$: The following Lyapunov function is considered:

$$V_\rho = V_{\rho-1} + \frac{1}{2}z_\rho^2 + \sum_{j=1}^{N}\frac{\tilde{\theta}_{\rho,j}^{\mathrm{T}}\tilde{\theta}_{\rho,j}}{2}$$

where $\tilde{\theta}_{\rho,j} = \theta_{\rho,j} - \hat{\theta}_{\rho,j}$ is the parameter estimation error of RBFNN, $\theta_{\rho,j}$ and $\hat{\theta}_{\rho,j}$ are the weight vector and its estimation.

By taking the derivative of V_ρ, we have

$$\begin{aligned}
\dot{V}_\rho ={}& \dot{V}_\rho + z_\rho z_{\rho+1} + z_\rho\alpha_\rho + z_\rho f_{\rho,l} - z_\rho\dot{\alpha}_{\rho-1} - \sum_{j=1}^{N}\tilde{\theta}_{\rho,j}^{\mathrm{T}}\dot{\hat{\theta}}_{\rho,j} \\
={}& \dot{V}_{\rho-1} + \frac{1}{2}z_\rho^2 + \frac{1}{2}z_{\rho+1}^2 + z_\rho\alpha_\rho + z_\rho F_{\rho,l} - \sum_{j=1}^{N}\tilde{\theta}_{\rho,j}^{\mathrm{T}}\dot{\hat{\theta}}_{\rho,j}
\end{aligned} \tag{20}$$

where $F_{\rho,l} = z_\rho + f_{\rho,l} - \dot{\alpha}_{\rho-1}$.

Obviously, $F_{\rho,l}$ is an unknown nonlinear function, which cannot be directly used for controller design. Therefore, according to Lemma 2.2, $F_{\rho,l}$ can be approximated by a RBFNN with the following form

$$F_{\rho,l}(S_\rho) = \theta_{\rho,l}^{\mathrm{T}}P_\rho(S_\rho) + \delta_{\rho,l}(S_\rho) \quad l \in \mathbb{N} \tag{21}$$

where $S_\rho = [x_1, \cdots, x_\rho, \hat{\theta}_{1,1}, \cdots, \hat{\theta}_{1,N}, \cdots, \hat{\theta}_{\rho-1,1}, \cdots \hat{\theta}_{\rho-1,N}]^{\mathrm{T}}$, $\theta_{\rho,l}$ is the ideal weight vector and $\delta_{\rho,l}$ is the approximation error satisfying $|\delta_{\rho,l}(S_\rho)| \le \delta_{\rho,l}^{*}$ with $\delta_{\rho,l}^{*}$ being a positive constant.

Substituting (21) into (20), we have

$$\begin{aligned}
\dot{V}_\rho \le{}& \dot{V}_{\rho-1} + \frac{1}{2}z_\rho^2 + \frac{1}{2}z_{\rho+1}^2 + z_\rho\alpha_\rho \\
&+ z_\rho\theta_{\rho,l}^{\mathrm{T}}P_\rho(S_\rho) + z_\rho\delta_{\rho,l} - \sum_{j=1}^{N}\tilde{\theta}_{\rho,j}^{\mathrm{T}}\dot{\hat{\theta}}_{\rho,j}
\end{aligned} \tag{22}$$

By repeating the procedure taken in Step 2, according to (22), the virtual control signal α_ρ and adaptive control law $\dot{\hat{\theta}}_{\rho,l}(t)$ are constructed as follows

$$\alpha_\rho = -\mu_\rho z_\rho - \sum_{j=1}^{N}\hat{\theta}_{\rho,j}^{\mathrm{T}}P_\rho(S_\rho) \tag{23}$$

$$\dot{\hat{\theta}}_{\rho,l}(t) = \omega_{l,\sigma(t)}(z_\rho(t_k)P_\rho(S_\rho(t_k)) - \sigma_{\rho,l}\hat{\theta}_{\rho,l}(t)) \tag{24}$$

where μ_2 and $\sigma_{2,l}$ are design positive parameters. Furthermore, it follows from (22) and (24) that

$$\sum_{j=1}^{N}\tilde{\theta}_{\rho,j}^{\mathrm{T}}\dot{\hat{\theta}}_{\rho,j} \le \tilde{\theta}_{\rho,l}^{\mathrm{T}}z_\rho(t_k)P_\rho(S_\rho(t_k)) - \sigma_{\rho,l}\tilde{\theta}_{\rho,l}^{\mathrm{T}}\theta_{\rho,l}(t) + \sum_{j=1}^{N}\sigma_{\rho,j}\tilde{\theta}_{\rho,j}^{\mathrm{T}}\tilde{\theta}_{\rho,j}(t) - \sum_{j=1,j\neq l}^{N}\sigma_{\rho,j}\tilde{\theta}_{\rho,j}^{\mathrm{T}}\tilde{\theta}_{\rho,j}(t) \tag{25}$$

Then, substituting (23), (24), and (25) into (22) yields

$$\begin{aligned}
\dot{V}_\rho \le{}& -\mu_1\xi^2 - \sum_{i=2}^{\rho}\mu_i z_i^2 + \frac{1}{2}z_{\rho+1}^2 - \sum_{i=1}^{\rho}\sum_{j=1}^{N}\sigma_{i,j}\tilde{\theta}_{i,j}^{\mathrm{T}}\tilde{\theta}_{i,j} \\
&+ \sqrt{2}\sqrt{V_\rho(t)}|\xi - \xi(t_k)| + \sqrt{2}\sqrt{V_\rho(t)}\sum_{i=2}^{\rho}|z_\rho - z_\rho(t_k)| \\
&+ \left(4\sqrt{2} + 4\rho - 4\right)\sqrt{V_\rho(t)}\sqrt{V_\rho(t_k)} + \zeta_{\rho,l}\sqrt{V_\rho(t)}
\end{aligned} \tag{26}$$

with $\zeta_{\rho,l} = \sqrt{2}\left(\sum_{j=1,j\neq l}^{N}(|\theta_{\rho,j}| + |\tilde{\theta}_{\rho,j}|) + \sigma_{\rho,l}|\theta_{\rho,l}| + \sum_{j=1,j\neq l}^{N}\sigma_{\rho,j}|\tilde{\theta}_{\rho,j}| + \delta_{\rho,l}^{*}\right) + \zeta_{\rho-1,l}$.

Step n: The following Lyapunov function is considered:

$$V_n = V_{n-1} + \frac{1}{2}z_n^2 + \sum_{j=1}^{N}\frac{\tilde{\theta}_{n,j}^{\mathrm{T}}\tilde{\theta}_{n,j}}{2}$$

where $\tilde{\theta}_{n,j} = \theta_{n,j} - \hat{\theta}_{n,j}$ is the parameter estimation error of RBFNN, $\theta_{n,j}$ and $\hat{\theta}_{n,j}$ are the weight vector and its estimation.

By taking the derivative of V_n, we have

$$\dot{V}_n = \dot{V}_{n-1} + z_n u + z_n f_{n,l}(x) - z_n \dot{\alpha}_{n-1} - \sum_{j=1}^{N} \tilde{\theta}_{n,j}^{\mathrm{T}} \dot{\hat{\theta}}_{n,j} \quad (27)$$

where $F_{n,l}(S_n) = \frac{1}{2} z_n + f_{n,l}(x) - \dot{\alpha}_{n-1}$.

Obviously, $F_{n,l}$ is an unknown nonlinear function, which cannot be directly used for controller design. Therefore, according to Lemma 2.2, $F_{n,l}$ can be approximated by a RBFNN with the following form

$$F_{n,l}(S_n) = \theta_{n,l}^{\mathrm{T}} P_n(S_n) + \delta_{n,l}(S_n) \quad l \in \mathbb{N} \quad (28)$$

where $S_n = [x_1, \cdots, x_n, \hat{\theta}_{1,1}, \cdots, \hat{\theta}_{1,N}, \cdots, \hat{\theta}_{n-1,1}, \cdots \hat{\theta}_{n-1,N}]^{\mathrm{T}}$, $\theta_{n,l}$, is the ideal weight vector and $\delta_{n,l}$ is the approximation error satisfying $|\delta_{n,l}(S_n)| \leq \delta_{n,l}^*$ with $\delta_{n,l}^*$ being a positive constant.

Substituting (28) into (27), we have.

$$\begin{aligned}\dot{V}_n \leq\ & \dot{V}_{n-1} + z_n(u - u^*) + z_n u^* + z_n \theta_{n,l}^{\mathrm{T}} P_n(S_n) \\ & + z_n \delta_{n,l} - \frac{1}{2} z_n^2 - \sum_{j=1}^{N} \tilde{\theta}_{n,j}^{\mathrm{T}} \dot{\hat{\theta}}_{n,j} \end{aligned} \quad (29)$$

According to (22), the actual control law u^* and adaptive control law $\dot{\hat{\theta}}_{n,l}(t)$ are constructed as follows

$$u^* = -\mu_n z_n - \hat{\theta}_{n,l}^{\mathrm{T}} P_n(S_n) \quad (30)$$

$$\dot{\hat{\theta}}_{n,l}(t) = \omega_{l,\sigma(t)}(z_n(t_k) P_n(S_n(t_k)) - \sigma_{n,l} \hat{\theta}_{n,l}(t)) \quad (31)$$

where μ_2 and $\sigma_{2,l}$ are design positive parameters.

Furthermore, according to (30), the sampled-data control law u can be constructed via CTD approach.

$$u(t_k) = -\mu_n z_n(t_k) - \hat{\theta}_{n,l}^{\mathrm{T}}(t_k) P_n(S_n(t_k)) \quad (32)$$

Then, substituting (31) and (32) into (29) yields

$$\begin{aligned}\dot{V}_n \leq\ & \dot{V}_{n-1} - \mu_n z_n^2 + z_n(u - u^*) + \sqrt{2}\sqrt{V_n(t)}\delta_{n,l}^* \\ & + \sqrt{2}\sqrt{V_n(t)}|z_n - z_n(t_k)| + 4\sqrt{V_n(t)}\sqrt{V_n(t_k)} \\ & + \sqrt{2}\sqrt{V_n(t)}\sigma_{n,l}|\theta_{n,l}| - \sum_{j=1}^{N} \sigma_{n,j} \tilde{\theta}_{n,j}^{\mathrm{T}} \tilde{\theta}_{n,j} \\ & + \sqrt{2}\sqrt{V_n(t)} \sum_{j=1, j\neq l}^{N} \sigma_{n,j}|\tilde{\theta}_{n,j}| \\ \leq\ & -\mu_1 \xi^2 - \sum_{i=2}^{n} \mu_i z_i^2 + z_n(u - u^*) \\ & - \sum_{i=1}^{n}\sum_{j=1}^{N} \sigma_{i,j} \tilde{\theta}_{i,j}^{\mathrm{T}} \tilde{\theta}_{i,j} + \sqrt{2}\sqrt{V_n(t)}|\xi - \xi(t_k)| \\ & + \sqrt{2}\sqrt{V_n(t)} \sum_{i=2}^{n} |z_i - z_i(t_k)| \\ & + \left(4\sqrt{2} + 4n - 4\right)\sqrt{V_n(t)}\sqrt{V_n(t_k)} + \zeta_{n,l}\sqrt{V_n(t)} \end{aligned} \quad (33)$$

with $\zeta_{n,l} = \sqrt{2}\left(\sum_{i=1}^{n-1}\sum_{j=1,j\neq l}^{N}(|\theta_{i,j}| + |\tilde{\theta}_{i,j}|) + \sum_{i=1}^{n} \sigma_{i,l}|\theta_{i,l}| + \sum_{i=1}^{n}\sum_{j=1,j\neq l}^{N} \sigma_{i,j}|\tilde{\theta}_{i,j}| + \sum_{i=1}^{n} \delta_{n,l}^*\right)$.

According to the above description, the following algorithm is summarised to illustrate the proposed control scheme.

Algorithm 1: The sampled-data Controller's Design

Input: The reference signal y_d and the system states $x_i(t_k)(1 \leq i \leq n)$
Step 1: Design the parameters ϕ_0, ϕ_∞ and λ of the prescribed performance function according to the performance requirements.
Step 2: Constructing Lyapunov function $V_i(1 \leq i \leq n-1)$. Select the parameters $\mu_1, \cdots \mu_{n-1}, \sigma_{i,1}, \cdots \sigma_{i,N}$, designing the virtual control signal $\alpha_i(1 \leq i \leq n-1)$ using (9) (16) (23) and adaptive control law $\dot{\hat{\theta}}_{i,l}(1 \leq i \leq n-1)$ using (10) (17) (24).
Step 3: Constructing Lyapunov function V_n. Select the parameters $\mu_n, \sigma_{n,1}, \cdots \sigma_{n,N}$, designing the actual control law u^* using (30) and adaptive control law $\dot{\hat{\theta}}_{n,l}$ using (31).
Step 4: Design the sampled-data controller for the system (1) in the form of (32) and calculate the sampling period T.
Output: $u(t_k)$

3.2 Stability analysis

Theorem 3.1: *Consider the switched nonlinear system (1) under Assumptions 2.1–2.2. If the virtual control signals are designed as (9), (16), (23) and the sampled controller is designed as (32) with the adaptive control laws designed as (10), (17), (24), and (31) under any switching signals, then all the signals in the closed-loop system are SGUUB and the tracking error achieves the prescribed performance.*

Proof: According to (33), we deduce

$$\begin{aligned}\dot{V}_n \leq\ & -cV_n + z_n(u - u^*) + \sqrt{2}\sqrt{V_n(t)}|\xi - \xi(t_k)| \\ & + \sqrt{2}\sqrt{V_n(t)}\sum_{i=2}^{n}|z_i - z_i(t_k)| + \zeta_n\sqrt{V_n(t)} \\ & + \left(4\sqrt{2} + 4n - 4\right)\sqrt{V_n(t)}\sqrt{V_n(t_k)} \end{aligned} \quad (34)$$

with $c = \min_{l\in\mathbb{N}}\{c_l\} > 0$, $c_l = \min\{4\mu_1, 2\mu_2, \cdots, 2\mu_n, 2\sigma_{i,1}, \cdots, 2\sigma_{i,N}\}$ and $\zeta_n = \max_{l\in\mathbb{N}}\{\zeta_{n,l}\}$.

Assume $Z(t) = [\xi, \phi, x_1 \cdots, x_n, \hat{\theta}_{1,1}, \cdots \hat{\theta}_{1,N}, \cdots, \hat{\theta}_{n,1}, \cdots \hat{\theta}_{n,N}]^{\mathrm{T}}, \forall t \in [t_k, t_{k+1})$, from Lemma 2.1, it can be obtained that

$$\begin{aligned}& ||Z(t) - Z(t_k)|| \\ & \leq \int_{t_k}^{t} \eta||Z(s) - Z(t_k)||ds + \eta(t - t_k)(||Z(t_k)|| + 1) \\ & \leq \bar{\eta}\left(\sqrt{V_{n,l}(t_k)} + 1\right)(e^{\eta(t-t_k)} - 1) \end{aligned} \quad (35)$$

where $\eta > 0$ and $\bar{\eta} > 0$ are constants.

From the previous process, it is clear that $|\xi - \xi(t_k)| \leq ||Z(t) - Z(t_k)||$, $|x_i(t) - x_i(t_k)| \leq ||Z(t) - Z(t_k)||$ and $|\hat{\theta}_{i,j}(t) - \hat{\theta}_{i,j}(t_k)| \leq ||Z(t) - Z(t_k)||$ hold. Next, we deduce $\forall t \in [t_k, t_{k+1})$

$$|u(t_k) - u^*(t)| \leq 2r_2\left(\sqrt{V_n(t_k)} + 1\right)(e^{\eta(t-t_k)} - 1) + 2r_1\bar{\theta}$$

$$+ 2\sqrt{2}r_1\sqrt{V_n(t_k)} \tag{36}$$

with $r_1 = \mu_n + \mu_n\mu_{n-1} + \cdots + \Pi_{i=1}^{n}\mu_i, r_2 = \bar{\eta}r_1$ and $\bar{\theta} = \max_{l\in\mathbb{N}}\left\{\sum_{i=1}^{n}|\theta_{i,l}|\right\}$.

Then, substituting (35) and (36) into (34) yields, for $\forall t \in [t_k, t_{k+1})$, we have

$$\begin{aligned}\dot{V}_n \le& \left(\left(4\sqrt{2}\gamma_2 + \sqrt{2}\bar{\eta}\right)e^{\eta(t-t_k)} - 4\sqrt{2}r_2 + 8r_1 - \sqrt{2}\bar{\eta}\right.\\ &\left.+ 4\sqrt{2} + 4n - 4\right)\sqrt{V_n(t)}\sqrt{V_n(t_k)}\\ &+ \sqrt{V_n(t)}\left(\left(4\sqrt{2}r_2 + \sqrt{2}\bar{\eta}\right)e^{\eta(t-t_k)} - 4\sqrt{2}r_2\right.\\ &\left.+ 4\sqrt{2}r_1\bar{\theta} + 2\sqrt{2}\zeta_n - \sqrt{2}\bar{\eta}\right)\\ \le& -cV_n + \sqrt{V_n(t)}\sqrt{V_n(t_k)}(r_3e^{\eta(t-t_k)} - r_4)\\ &+ \sqrt{V_n(t)}(r_3e^{\eta(t-t_k)} - r_5)\end{aligned} \tag{37}$$

with $r_3 = 4\sqrt{2}r_2 + \sqrt{2}\bar{\eta}$, $r_4 = r_3 - 8r_1 - 4n - 4\sqrt{2} + 4$ and $r_5 = r_3 - 4\sqrt{2}r_1\bar{\theta} - \zeta_n$.

Since $W(t) = \sqrt{V_n(t)}$, from (37), we have

$$\dot{W}(t) \le -\beta_1 W(t) + r_6 W(t_k) + r_7 \forall t \in [t_k, t_{k+1}) \tag{38}$$

with $\beta_1 = c/2, r_6 = \frac{r_3e^{\eta T} - r_4}{2}$ and $r_7 = \frac{r_3e^{\eta T} - r_5}{2}$

Subsequently, from (38), we deduce

$$W(t) \le \beta_2 W(t_k) + \varphi \forall t \in [t_k, t_{k+1})$$

with $\beta_2 = e^{-\beta_1 T} + \gamma_6(1 - e^{-\beta_1 T})/\beta_1$ and $\varphi = \gamma_7(1 - e^{-\beta_1 T})/\beta_1$.

Since $t = t_{k+1}$, the following form can be obtained.

$$W(t_{k+1}) \le \beta_2 W(t_k) + \varphi, \forall t \in [t_k, t_{k+1}) \tag{39}$$

In order to guarantee $\beta_2 \in (0, 1)$, we choose the sampling period

$$T < \frac{1}{\eta}\ln\left(\frac{r_4 + 2\beta_1}{r_3}\right) \tag{40}$$

Then, according to (39), we have

$$W(t_{k+1}) \le \beta_2^k W(0) + \varphi\left(\frac{1}{1-\beta_2}\right) \tag{41}$$

According to (41), it can deduce,

$$W(t) \le W(0) + \frac{\varphi}{1-\beta_2} \tag{42}$$

Then, the following inequality holds.

$$\begin{aligned}\frac{1}{4}\xi^2 =& \frac{1}{4}\left(\frac{(y-y_d)^2}{\phi^2(t) - (y(t) - y_d(t))^2}\right)^2\\ &\le V(t) \le W^2(t) \le \left(W(0) + \frac{\varphi}{1-\beta_2}\right)^2\end{aligned} \tag{43}$$

Meanwhile, we have

$$\begin{aligned}&\left(1 - \left(W(0) + \frac{\varphi}{1-\beta_2}\right)^2\right)(y-y_d)^4\\ &\le 4\left(W(0) + \frac{\varphi}{1-\beta_2}\right)^2(\phi^4 - 2\phi^2(y-y_d)^2)\end{aligned} \tag{44}$$

Based on (43) and (44), the following inequality holds through selecting appropriate initial conditions and design parameters

$$1 - \left(W(0) + \frac{\varphi}{1-\beta_2}\right)^2 \ge 0 \tag{45}$$

$$\phi^4 - 2\phi^2(y-y_d)^2 \ge 0 \tag{46}$$

Thus, the tracking error is limited to the range of the performance function. That is

$$|y - y_d| \le \frac{\varphi}{\sqrt{2}} \le \varphi \tag{47}$$

Above all, it can guarantee that all signals of the closed-loop system are SGUUB and that the tracking error achieves the prescribed performance under any switching period. Theorem 3.1 is proven to be complete. ■

Remark 3.1: The design of the controller parameters has a significant impact on the performance of the controller. The control effect is significantly improved when the parameters μ_i and $\sigma_{i,l}$ are increased. However, when the parameters exceed a specific value, the system output will fluctuate, and the control effect will be reduced. Therefore, it is necessary to be careful when designing the controller parameters to prevent irreversible damage.

Remark 3.2: In fact, there exists approximation error when using NNs to approximate nonlinear functions. Therefore, the proposed NN-based control strategy can only ensure the system state satisfies SGUUB rather than globally asymptotically stable.

4. Simulation examples

In this section, two examples are given to demonstrate the effectively of the proposed adaptive sampled-data control method.

Example 4.1: Consider the following switched nonlinear system containing two subsystems

$$\begin{cases}\dot{x}_1 = x_2 + f_{1,\sigma(t)}(x_1)\\ \dot{x}_2 = u + f_{2,\sigma(t)}(\bar{x}_2)\\ y = x_1\end{cases} \tag{48}$$

where $\sigma(t) : [0, \infty) \to \mathbb{N} = \{1, 2\}, f_{1,1}(x_1) = -2x_1e^{-0.5x_1}, f_{2,1}(\bar{x}_2) = \cos(x_1)\sin(x_2), f_{2,1}(x_1) = -2\sin(x_1)e^{-0.5x_1}, f_{2,1}(\bar{x}_2) = \sin(x_1)\cos(x_2)$, The initial states of the system are $x_1(0) = 0.5$ and $x_2(0) = 0.5$..u is the control signal. The reference signal is selected as $y_d = 0.1\sin(0.5t)$.

During the simulation, the design parameters of the prescribed performance function are selected as $\phi_0 = 5$, $\phi_\infty = 0.1$ and $\lambda = 2.5$. According to Theorem 3.1, the virtual control signal α_1 and the adaptive control law $\dot{\hat{\theta}}_{1,l}(t)$ of the system (48) are

$$\alpha_1 = -\frac{1}{\varsigma}(\mu_1\xi + \hat{\theta}_{1,1}^{\mathrm{T}}P_1(S_1) + \hat{\theta}_{1,2}^{\mathrm{T}}P_1(S_1)) \tag{49}$$

$$\dot{\hat{\theta}}_{1,l}(t) = \omega_{l,\sigma(t)}(\xi(t_k)P_1(S_1(t_k)) - \sigma_{1,l}\hat{\theta}_{1,l}(t)) \tag{50}$$

Meanwhile, in combination with the backstepping design method, the control input u and the adaptive control law $\dot{\hat{\theta}}_{1,l}(t)$ of the system (48) is

$$u = -\mu_2 z_2(t_k) - \hat{\theta}^{\mathrm{T}}_{2,\sigma(t)}(t_k)P_2(S_2(t_k)) \tag{51}$$

$$\dot{\hat{\theta}}_{n,l}(t) = \omega_{l,\sigma(t)}(z_n(t_k)P_n(S_n(t_k)) - \sigma_{n,l}\hat{\theta}_{n,l}(t)) \tag{52}$$

where $S_1 = [x_1]^{\mathrm{T}}$ and $S_2 = [x_1, x_2\hat{\theta}_{1,1}, \hat{\theta}_{1,2}]^{\mathrm{T}}$. There are 7 nodes whose centre is located in $[-3, 3]$ and widths being equal to 0.2 in the first RBF vector. There are 36 nodes whose centre is located in $[-9, 9] \times [-9, 9] \times [-9, 9] \times [-9, 9]$ and widths being equal to 0.2. The controller parameters are taken as $\mu_1 = 16$ and $\mu_2 = 5$. And the sampling period is chosen as 0.1. The simulation results are shown in Figures 1–5.

Figure 1 shows the result of the output signal y tracking the reference signal y_d. Figure 2 shows the tracking error and the boundary via the prescribed performance function, which is show that the tracking error always satisfies the prescribed performance and converges quickly to near the origin. Figure 3 shows the control input based on the sampled-data control, which changes only at the sampling moment. Figure 4 shows the system states x_1 and x_2 are bounded. Figure 5 displays the specific switching signal for the simulation process.

In addition, Figures 6–7 show the effects of controller parameters and neural network coefficients on the control performance.

In Figure 6, it is clear that the control parameters have a significant effect on the control performance. The control performance changes dramatically when the parameter k_1 is altered. Increasing k_1, the control performance gradually changes until k_1 reaches a value, and the control performance start to weaken and fluctuate. When the parameter k_2 is changed, the control performance changes slightly. Increasing k_2, the control performance gradually improves until k_2 exceeds a value, and the control effect does not change much.

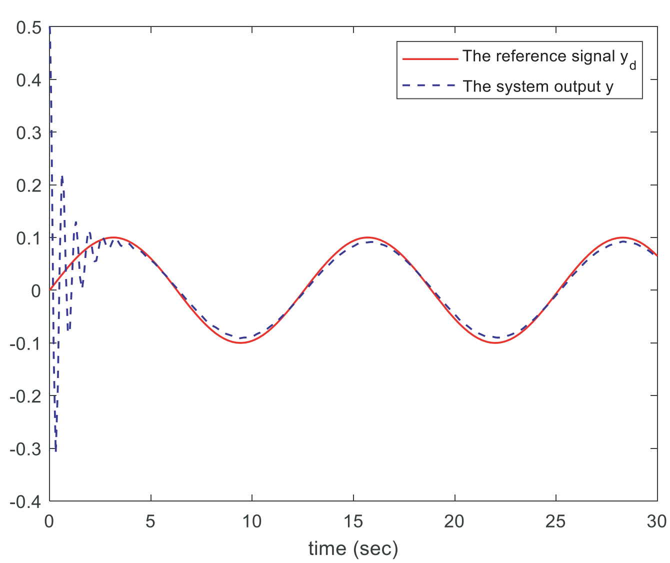

Figure 1. The system output y and the reference signal y_d.

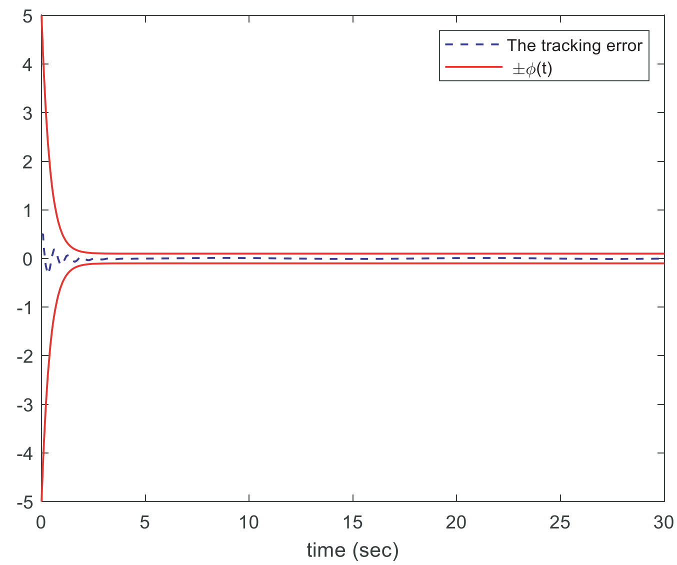

Figure 2. The tracking error and the prescribed performance function $\phi(t)$.

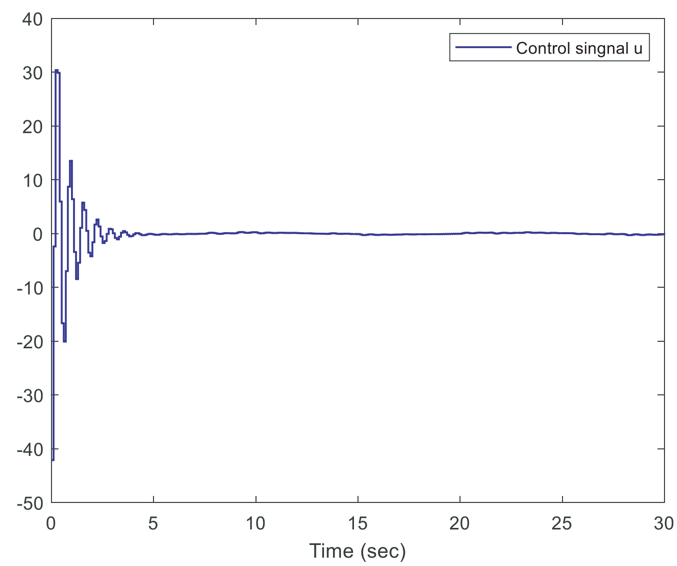

Figure 3. The control signal $u(t)$.

In Figure 7, we can obtain that the number of neural network nodes has little effect on the control performance, and the width has some impact on the control performance. However, increasing the number of neural network nodes add the complexity of computer computation and the training time of the control strategy.

Example 4.2: To further demonstrate the value of our proposed control scheme in the practical control system, consider a practical engineering MSD with controller switching. According to (L i et al., 2018), its mathematical can be specifically expressed as follows

$$\begin{cases} \dot{x}_1 = x_2 \\ \dot{x}_2 = u - \dfrac{1}{m}[f(x_1) + \Delta f_{\sigma(t)}(x) + g(x_2)] \\ y = x_1 \end{cases} \tag{53}$$

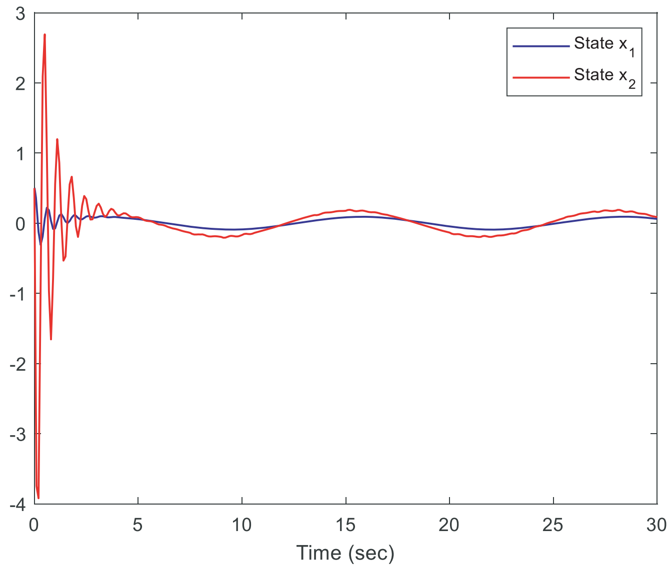

Figure 4. The state variable x_1 and the state variable x_2.

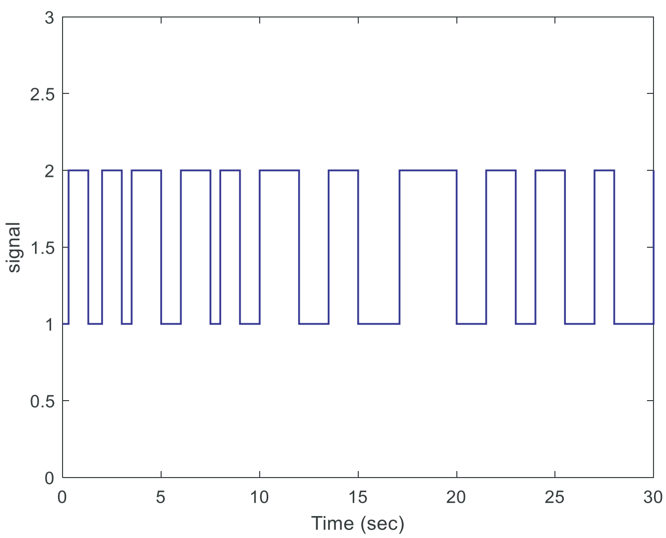

Figure 5. The switching signal.

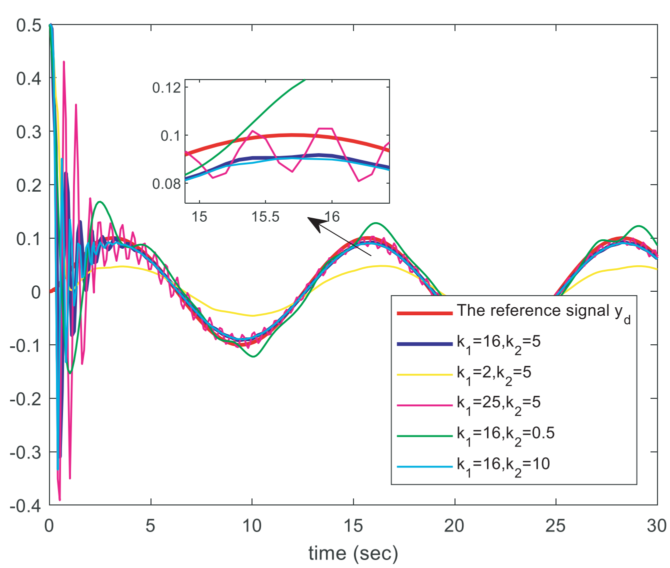

Figure 6. The impact of different controller parameters on the tracking performance.

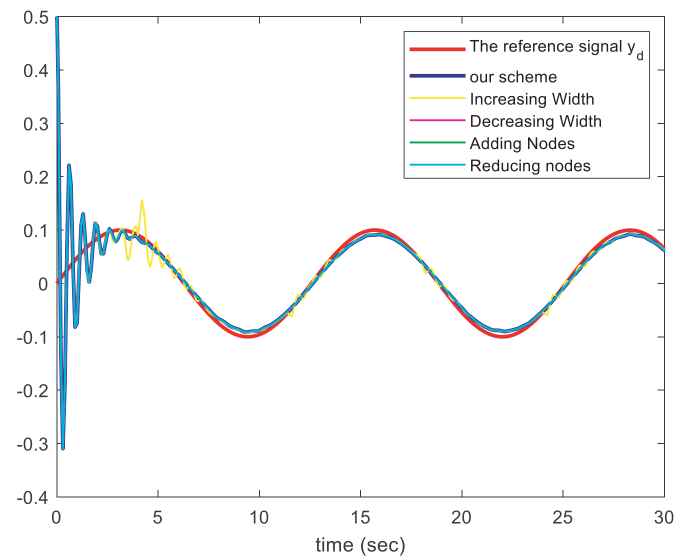

Figure 7. The impact of different RBFNN parameters on the tracking performance.

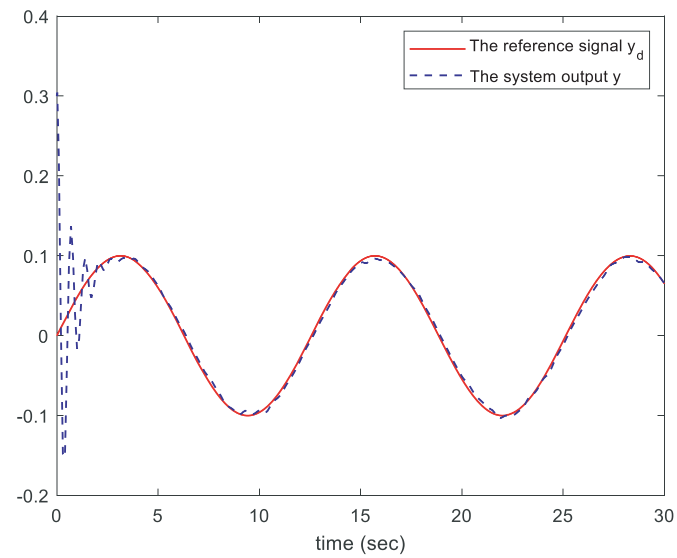

Figure 8. The output y and the reference signal y_d of MSD system.

where $\sigma(t) : [0, \infty) \to \mathbb{N} = \{1, 2\}$, $m = \frac{1}{3}$, $f(x_1) = 2x_1^2$, $g(x_2) = 0.5x_2$, $\Delta f_1(x) = x_1 \cos(x_2^2)$, $\Delta f_2(x) = e^{x_2^2} \sin(x_1^2)$, The initial state of the system are $x_1(0) = 0.3$ and $x_2(0) = 0.5$.. u is the control signal. The reference signal is $y_d = 0.1 \sin(0.5t)$.

In simulation, the parameters of the prescribed performance function are selected as $\phi_0 = 5$, $\phi_\infty = 0.1$ and $\lambda = 2.5$. The controller parameters are taken as $\mu_1 = 15$ and $\mu_2 = 5$. And the sampling period is chosen as 0.1. The simulation results are shown in Figures 8–12.

In the MSD system, Figure 8 shows the tracking performance of the output signal. Figure 9 shows that the tracking error is always limited to satisfy the prescribed performance function. With the control signal in Figure 10 and the switching signal in Figure 12, the tracking error quickly converges near the origin. Figure 11 displays the MSD system states, x_1 and x_2, are both bounded.

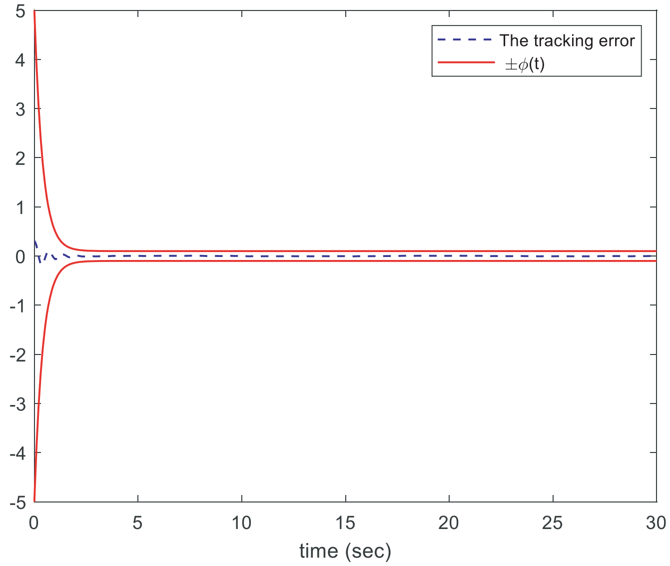

Figure 9. The tracking error of the MSD system and the prescribed performance function $\phi(t)$.

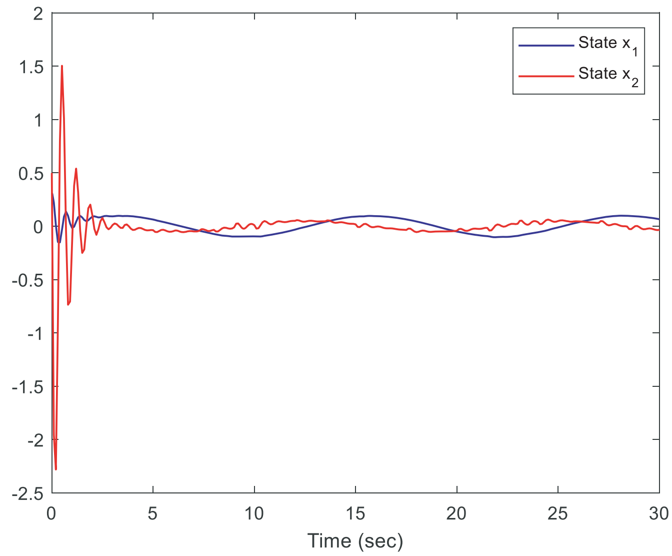

Figure 11. The state variable x_1 and the state variable x_2 of MSD system.

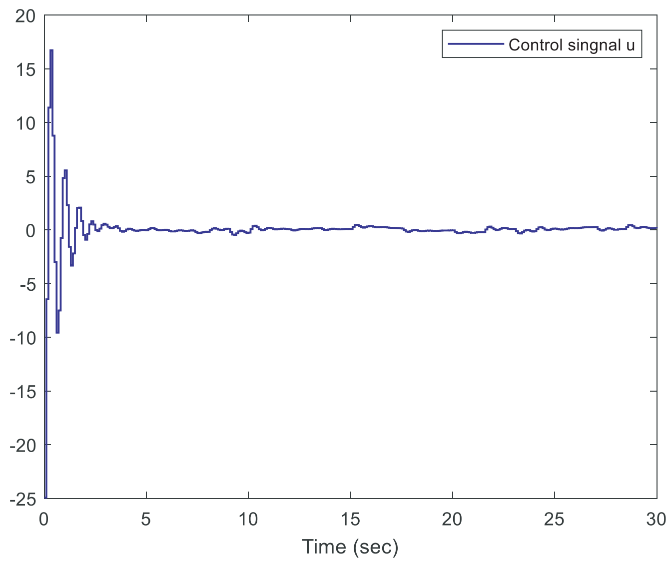

Figure 10. The control signal $u(t)$ of MSD system.

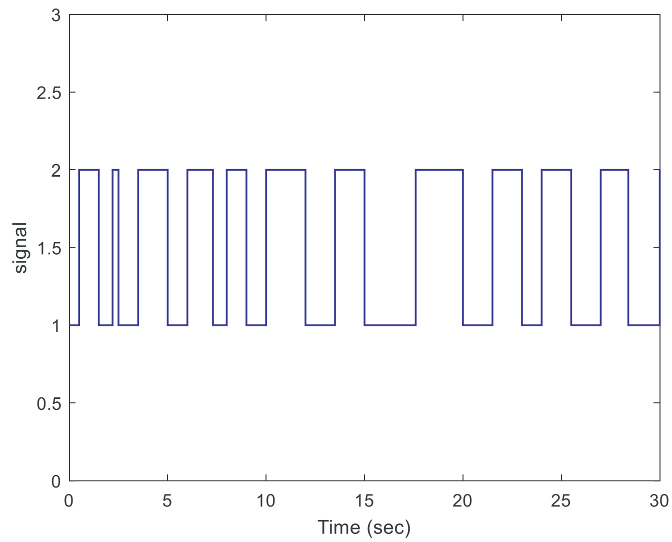

Figure 12. The switching signal of MSD system.

From the simulation results, the control scheme designed in this paper has been controlled well in both Example 4.1 and Example 4.2. And the controller structure is simple, which is of great significance for solving the problem of sampled-data adaptive tracking control for switched nonlinear systems with prescribed performance.

5. Conclusion

In this paper, a novel adaptive sample-data control approach is proposed to address the tracking problem for a class of switched nonlinear systems with prescribed performance. Firstly, a coordinate transformation is constructed to satisfy the prescribed performance requirements. Secondly, by using RBFNNs and the backstepping technique, the adaptive control signal and the adaptive laws are obtained. Thirdly, the limitation of the sampling period is derived from stability analysis. Finally, it can be proven that all closed-loop signals are SGUUB, and the tracking error is always within the range of prescribed performance requirements. Two simulation examples, one numerical and one practical, validate the effectiveness of our proposed strategy.

Disclosure statement

No potential conflict of interest was reported by the authors.

Funding

This work was supported by the Shandong Provincial Natural Science Foundation, China [ZR2020QF055].

ORCID

Si-Min Liu http://orcid.org/0000-0002-8243-4026
Yu-Qun Han http://orcid.org/0000-0002-9055-2954

References

Chen, Y. X., Liu, Z., Chen, C. L. P., & Zhang, Y. (2021). Adaptive fuzzy control of switched nonlinear systems with uncertain dead-zone: A mode-dependent fuzzy dead-zone model. *Neurocomputing*, *432*, 133–144. https://doi.org/10.1016/j.neucom.2020.12.044

Cui, D., Zou, W. C., Guo, J., & Xiang, Z. R. (2022). Neural network-based adaptive finite-time tracking control of switched nonlinear systems with time-varying delay. *Applied Mathematics and Computation*, *428*, 127216. https://doi.org/10.1016/j.amc.2022.127216

Guan, C. X., Chen, W. Z., Yang, L., & Fei, Z. Y. (2022). Sampled-data asynchronous control for switched nonlinear systems with relaxed switching rules. *IEEE Transactions on Cybernetics*, *52*(11), 11549–11560. https://doi.org/10.1109/TCYB.2021.3079308

Huang, Y. B., Na, J., & Wu, X. (2015). Adaptive control of nonlinear uncertain active suspension systems with prescribed performance. *ISA Transactions*, *54*, 145–155. https://doi.org/10.1016/j.isatra.2014.05.025

Jin, Y., Fu, J., Zhang, Y. M., & Jing, Y. W. (2014). Reliable control of a class of switched cascade nonlinear systems with its application to flight control. *Nonlinear Analysis: Hybrid Systems*, *11*, 11–21. https://doi.org/10.1016/j.nahs.2013.03.003

Lai, G. Y., Liu, Z., Zhang, Y., Philip Chen, C. L., & Xie, S. L. (2018). Adaptive backstepping-based tracking control of a class of uncertain switched nonlinear systems. *Automatica*, *91*, 301–310. https://doi.org/10.1016/j.automatica.2017.12.008

Li, S., Ahn, C. K., Guo, J., & Xiang, Z. R. (2021). Neural network-based sampled-data control for switched uncertain nonlinear systems. *IEEE Transactions on Systems, Man, and Cybernetics: Systems*, *51*(9), 5437–5445. https://doi.org/10.1109/TSMC.2019.2954231

Li, S., Ahn, C. K., & Xiang, Z. R. (2019). Sampled-data adaptive output feedback fuzzy stabilization for switched nonlinear systems with asynchronous switching. *IEEE Transactions on Fuzzy Systems*, *27*(1), 200–205. https://doi.org/10.1109/TFUZZ.2018.2881660

Li, S., Guo, J., & Xiang, Z. (2019). Global stabilization of a class of switched nonlinear systems under sampled-data control. *IEEE Transactions on Systems, Man, and Cybernetics: Systems*, *49*(9), 1912–1919. https://doi.org/10.1109/TSMC.2018.2836930

Li, S., Guo, J., & Xiang, Z. R. (2018). Sampled-data adaptive prescribed performance control of a class of nonlinear systems. *Neurocomputing*, *283*, 282–292. https://doi.org/10.1016/j.neucom.2018.01.026

Li, W. F., Xie, Z. C., Cao, Y. C., Wong, P. K., & Zhao, J. (2021). Sampled-data asynchronous fuzzy output feedback control for active suspension systems in restricted frequency domain. *IEEE/CAA Journal of Automatica Sinica*, *8*(5), 1052–1066. https://doi.org/10.1109/JAS.2020.1003306

Li, Y. M., & Tong, S. C. (2015). Prescribed performance adaptive fuzzy output-feedback dynamic surface control for nonlinear large-scale systems with time delays. *Information Sciences*, *292*, 125–142. https://doi.org/10.1016/j.ins.2014.08.060

Li, Y. M., Tong, S. C., Liu, L., & Feng, G. (2017). Adaptive output-feedback control design with prescribed performance for switched nonlinear systems. *Automatica*, *80*, 225–231. https://doi.org/10.1016/j.automatica.2017.02.005

Li, Y. M., & Yu, K. T. (2022). Adaptive fuzzy decentralized sampled-data control for large-scale nonlinear systems. *IEEE Transactions on Fuzzy Systems*, *30*(6), 1809–1822. https://doi.org/10.1109/TFUZZ.2021.3069321

Li, Z. J., & Zhao, J. (2021). Adaptive consensus of non-strict feedback switched multi-agent systems with input saturations. *IEEE/CAA Journal of Automatica Sinica*, *8*(11), 1752–1761. https://doi.org/10.1109/JAS.2021.1004165

Lian, J., & Li, C. (2020). Event-triggered control for a class of switched uncertain nonlinear systems. *Systems & Control Letters*, *135*, 104592. https://doi.org/10.1016/j.sysconle.2019.104592

Liu, L., Chen, A. Q., & Liu, Y. J. (2022). Adaptive fuzzy output-feedback control for switched uncertain nonlinear systems with full-state constraints. *IEEE Transactions on Cybernetics*, *52*(8), 7340–7351. https://doi.org/10.1109/TCYB.2021.3050510

Liu, Y. C., Zhu, Q. D., & Zhao, N. (2021). Event-triggered adaptive fuzzy control for switched nonlinear systems with state constraints. *Information Sciences*, *562*, 28–43. https://doi.org/10.1016/j.ins.2021.01.030

Ma, L., Xu, N., Huo, X., & Zhao, X. D. (2020). Adaptive finite-time output-feedback control design for switched pure-feedback nonlinear systems with average dwell time. *Nonlinear Analysis: Hybrid Systems*, *37*, 100908. https://doi.org/10.1016/j.nahs.2020.100908

Ma, Z. Y., & Ma, H. J. (2020). Decentralized adaptive NN output-feedback fault compensation control of nonlinear switched large-scale systems with actuator dead-zones. *IEEE Transactions on Systems, Man, and Cybernetics: Systems*, *50*(9), 3435–3447. https://doi.org/10.1109/TSMC.2018.2867948

Meng, X., Zhai, D., Fu, Z. M., & Xie, X. P. (2020). Adaptive fault tolerant control for a class of switched nonlinear systems with unknown control directions. *Applied Mathematics and Computation*, *370*, 124913. https://doi.org/10.1016/j.amc.2019.124913

Ming, C., Sun, R. S., & Zhu, B. (2017). Nonlinear fault-tolerant control with prescribed performance for air-breathing supersonic missiles. *Journal of Spacecraft and Rockets*, *54*(5), 1092–1099. https://doi.org/10.2514/1.A33721

Niu, B., Ahn, C. K., Li, H., & Liu, M. (2018). Adaptive control for stochastic switched nonlower triangular nonlinear systems and its application to a one-link manipulator. *IEEE Transactions on Systems, Man, and Cybernetics: Systems*, *48*(10), 1701–1714. https://doi.org/10.1109/TSMC.2017.2685638

Niu, B., Liu, Y. J., Zhou, W. L., Li, H. T., Duan, P. Y., & Li, J. Q. (2020). Multiple Lyapunov functions for adaptive neural tracking control of switched nonlinear nonlower-triangular systems. *IEEE Transactions on Cybernetics*, *50*(5), 1877–1886. https://doi.org/10.1109/TCYB.2019.2906372

Niu, B., Wang, D., Liu, M., Song, X. M., Wang, H. Q., & Duan, P. Y. (2020). Adaptive neural output-feedback controller design of switched nonlower triangular nonlinear systems with time delays. *IEEE Transactions on Neural Networks and Learning Systems*, *31*(10), 4084–4093. https://doi.org/10.1109/TNNLS.2019.2952108

Sanner, R. M., & Slotine, J. E. (1992). Gaussian networks for direct adaptive control. *IEEE Transactions on Neural Networks*, *3*(6), 837–863. https://doi.org/10.1109/72.165588

Sheng, Z. L., Lin, C., Chen, B., & Wang, Q. G. (2022). Stability analysis of sampled-data systems via novel Lyapunov functional method. *Information Sciences*, *585*, 559–570. https://doi.org/10.1016/j.ins.2021.11.071

Su, Z. G., Qian, C. J., Hao, Y. S., & Zhao, M. (2018). Global stabilization via sampled-data output feedback for large-scale systems interconnected by inherent nonlinearities. *Automatica*, *92*, 254–258. https://doi.org/10.1016/j.automatica.2018.03.057

Sui, S., Tong, S. C., & Li, Y. M. (2015). Observer-based fuzzy adaptive prescribed performance tracking control for nonlinear stochastic systems with input saturation. *Neurocomputing*, *158*, 100–108. https://doi.org/10.1016/j.neucom.2015.01.063

Tang, L., & Zhao, J. (2017). Neural network based adaptive prescribed performance control for a class of switched nonlinear systems. *Neurocomputing*, *230*, 316–321. https://doi.org/10.1016/j.neucom.2016.12.011

Wang, F., Chen, B., Lin, C., Zhang, J., & Meng, X. Z. (2018). Adaptive neural network finite-time output feedback control of quantized nonlinear systems. *IEEE Transactions on Cybernetics*, *48*(6), 1839–1848. https://doi.org/10.1109/TCYB.2017.2715980

Wang, F. L., & Long, L. J. (2022). Switched-observer-based event-triggered adaptive fuzzy funnel control for switched nonlinear systems. *IEEE Transactions on Fuzzy Systems*, *30*(6), 1773–1787. https://doi.org/10.1109/TFUZZ.2021.3067063

Wang, H. Q., Zou, Y. C., Liu, P. X. P., & Liu, X. P. (2018). Robust fuzzy adaptive funnel control of nonlinear systems with dynamic uncertainties. *Neurocomputing*, *314*, 299–309. https://doi.org/10.1016/j.neucom.2018.06.053

Wu, X., Zhang, K. J., & Cheng, M. (2018). Optimal control of constrained switched systems and application to electrical vehicle energy management. *Nonlinear Analysis: Hybrid Systems*, *30*, 171–188. https://doi.org/10.1016/j.nahs.2018.05.006

Zeng, D. P., Liu, Z., Chen, C. L. P., & Zhang, Y. (2021). Adaptive neural tracking control for switched nonlinear systems with state quantization. *Neurocomputing*, *454*, 392–404. https://doi.org/10.1016/j.neucom.2021.02.083

Zhai, D., An, L. W., Dong, J. X., & Zhang, Q. L. (2018). Switched adaptive fuzzy tracking control for a class of switched nonlinear systems under arbitrary switching. *IEEE Transactions on Fuzzy Systems*, *26*(2), 585–597. https://doi.org/10.1109/TFUZZ.2017.2686378

Zhang, L. L., Zhu, L. C., Hua, C. C., & Qian, C. (2021). Adaptive neural network control for a class of interconnected pure-feedback time-delay nonlinear systems with full-state constraints and unknown measurement sensitivities. *Neurocomputing*, *461*, 147–161. https://doi.org/10.1016/j.neucom.2021.07.043

Zhang, T., & Xiao, S. P. (2020). Stability analysis of sampled-data control system and its application to electric power market. *Chinese Journal of Electrical Engineering*, *6*(1), 61–70. https://doi.org/10.23919/CJEE.2020.000005

Zhang, W. H., & Wei, W. (2021). Disturbance-observer-based finite-time adaptive fuzzy control for non-triangular switched nonlinear systems with input saturation. *Information Sciences*, *561*, 152–167. https://doi.org/10.1016/j.ins.2021.01.026

Zhu, S. L., & Han, Y. Q. (2022). Adaptive decentralized prescribed performance control for a class of large-scale nonlinear systems subject to nonsymmetric input saturations. *Neural Computing and Applications*, *34*(13), 11123–11140. https://doi.org/10.1007/s00521-022-07032-8